Automatic quantification of liver-heart cross talk for quality assessment in SPECT myocardial perfusion imaging

Guo-Qing Wei [a], Anant Madabushi [b], JianZhong Qian [a], and John Engdahl [c]

[a] Imaging Department, Siemens Corporate Research, Inc.
755 College Road East, Princeton NJ 08536
[b] Department of Bioengineering,
University of Pennsylvania, Philadelphia, PA 19104
[c] Siemens Medical Solutions, Inc.
2501 North Barrington Road, Hoffman Estates, IL 60195

ABSTRACT

In the single-photon emission computed tomography (SPECT), it is highly desirable to provide physicians with a measure of the strength of the liver-heart cross talk as a means of assessing the quality of the images, so that appropriate actions can be taken to avoid false diagnosis. Liver-heart cross talk is an phenomenon in which the liver count interferes with the heart count in 3D reconstruction, which generates artifacts in the reconstructed images. In this paper, we propose an automatic method for quantification of such liver-heart cross talk. The system performs heart detection followed by non-heart organ segmentation and quantification of their activities. An appearance-based approach is applied to find the heart center in each image, with invariance to image intensity and contrast. Then heart and non-heart activities are quantified in each image. A measurement formula is proposed to compute the amount of liver-heart cross talk as a function of the size of the non-heart activity regions, of the strengths of the heart and non-heart activities, and of the distance of the non-heart regions to the heart. The method has been tested on 150 patient studies of different isotopes and acquisition types, with very promising results.

Keywords: SPECT, liver-heart cross talk, quality number, heart detection, robust fitting, non-heart activity segmentation, non-heart activity quantification, fusion.

1. INTRODUCTION

In the single-photon emission computed tomography (SPECT) of nuclear medicine, there are many factors that may cause artifacts in the reconstruction of the heart. Among them are attenuation [1], position dependent resolution [2], Compton scatter [2], motion [13,4], and liver uptake [6]. Although correction algorithms exist for most of the artifacts mentioned above, these algorithms themselves may cause additional artifacts or side effects when applied inappropriately. Therefore it is highly necessary to provide an automatic measurement system to quantify the severity of each artifact, so that a corresponding correction algorithm is applied only when the degree of severity is above a certain threshold. In this paper, we attempt to quantify one of the least studied artifacts in SPECT, namely the artifact caused by liver uptakes.

Germanto *et al.* [6] first pointed out that the filtered back-projection algorithm (FBP) [5], which is the most widely used method for heart reconstruction, produces artifactual defects in the inferior/inferoseptal myocardial wall when there are the high uptakes of either liver activities or of other organs. This is reflected in the reduced count in the myocardial wall near the liver. This phenomenon is often called the *liver-heart cross talk.* A direct consequence of that is that this liver-heart artifact may be confused with artifacts of coronary artery diseases, causing false diagnosis by physicians. To remedy this problem, it was suggested in [6] that FBP be performed using a ramp filter and without pre-smoothing of the projection data. Nuyts *et al.* [7] found that the Maximum-Likelihood Expectation-Maximization (ML-EM) algorithm [8] is capable of suppressing the artifacts. If an accurate attenuation map is available, the ML-EM algorithm can nearly eliminate the artifact [7]. The ML-EM algorithm, however, is much slower than the FBP algorithm and some times has problems in convergence. Therefore, it should be applied only when it is needed.

Medical Imaging 2002: Image Processing, Milan Sonka, J. Michael Fitzpatrick,
Editors, Proceedings of SPIE Vol. 4684 (2002) © 2002 SPIE · 1605-7422/02/$15.00

Based on the above analysis, it is highly desirable to devise a method to monitor the liver-heart artifact automatically. The method should give a quantitative measurement about the extent to which the cross talk may be occurring. Therefore based on this quality number, physicians can take appropriate actions, e.g., to switch to the ML-EM algorithm.

2. METHODOLOGY

The first step in quantifying the liver-heart cross-talk is to localize the heart position in each image. Based on the heart position and count, liver activities are then segmented and quantified. A flowchart of the system diagram is shown in Fig.1.

2.1. Heart detection

2.1.1. Region of interest determination

To find the heart position in each image, it is imperative to restrict the search region to some region of interest (ROI), so that not only search time can be substantially reduced, but also a more robust detection can be achieved. In [10], a technique is described to find an upper limit and a lower limit of the heart in the vertical direction of the images. This is based on the 1-D pseudo motion analysis of the image sequence. Since the heart pixels are usually the brightest points in the corresponding scan line, and since the heart follow a fixed pattern of motion, such information can be encoded in a 1D curve called the pseudo motion map. First, the pseudo motion map of an identified heart is extracted as a template. Then this template is matched against the pseudo motion maps of the scan lines. A correlation profile is thus obtained. The scan lines containing the heart produce higher correlation scores than the others.

Since SPECT images are very noisy, the correlation profile obtained may contain high correlation scores that are non-heart. Also, some scan lines containing the heart may produce low correlations. To remove the false peaks and to fill the gaps in the correlation profile, morphological closing operation is performed. The obtained profile is then thresholded to find connected components (segments). Since the approximate heart size is known *a priori*, the segments whose sizes are above a pre-selected threshold or below another pre-selected threshold are discarded. The remaining segments represent possible heart positions in the image sequence.

We also extended the method of [10] by refining the region of interest for each frame independently. In the 1D pseudo motion map, the value at an image frame represents the x-coordinate of the brightest point in the scan line. This information can be used to define the heart range along the x-axis for each frame. Since the maximum intensity on a scan line containing the heart may be not from the heart, errors may occur in determining the x-range of the heart. There are two sources of errors. First, noises may alter the heart count. We use smoothing operations to reduce errors of this kind. Secondly, high liver activity may occur on the same scan line of the heart. In this case, the maximum intensity may be from the liver, instead of the heart. We do not try to avoid errors of this kind at the ROI localization. Instead, we expect the trajectory fitting in the heart detection phase to discard false localization of heart.

2.1.2. Heart detection by a training-based method

The heart detection is based on two steps: off-line training and on-line detection. In the off-line stage, typical heart images are extracted manually. Eigen-heart images are then found by principal component analysis (PCA). In contrast to conventional methods of PCA-based training, there is no brightness and contrast normalization since such normalization is usually based on maximum and minimum intensity values and is very sensitive to noises (SPECT images are very noisy). In the detection stage, an integrated approach is proposed to shift and scale the image under consideration to fit the intensity range of the eigen-images. This is achieved by projecting the intensity-transformed image (with unknown scale and shift parameters) onto the eigen-images and minimizing the error of fit. This leads to a set of equations on both the intensity transformation parameters and the projection coefficients. Based on the orthonormality properties of the eigen-images, these equations can be reduced to a set of linear equations on scale and shift parameters only. By using the least-squares method, these equations can be easily solved for the scale and shift parameters. In this way, the normalization is made robust against noises. Details of the method are presented in [11].

2.1.3. Heart position fitting and refining

The heart positions are detected in each frame independently as described in section 2.1.2. It is known from SPECT imaging, however, that the heart trajectory should follow a sine curve due to the pattern of camera motions. This prior knowledge can be used to correct detection errors in individual frames. Suppose $\{(x_i, y_i), i = 1,2,...N\}$ are the coordinates of the detected heart positions. Then the x-coordinates should satisfy a sine curve

$$x_i = A \sin(ki + \theta) \tag{1}$$

where $A, k,$ and θ are the parameters of the sine curve. We fit the x-coordinates of the detected heart positions by minimizing the following error function

$$E = \sum_{i=1}^{N} \rho_i(d_i)\, d_i^{\,2} \tag{2}$$

$$d_i = x_i - A\sin(kx_i + \theta) \tag{3}$$

with respect to the parameters $A, k,$ and θ, where $\rho(d)$ is a weighting function used to exclude outliers, outliers being detected positions whose errors are too large to satisfy a sine curve; d_i is the error of fit for the i-th image. The function $\rho(d)$ is chosen such that when the error d becomes larger, the weight becomes less:

$$\rho(d) = e^{-d^2/\sigma^2} \tag{4}$$

In this way, frames in which the errors of heart positions are too large will have negligible effect on the final fitting result; that is, the fitting is mainly based on the heart positions which satisfy a sine trajectory. The minimization of (2) over $A, k,$ and θ is achieved iteratively as follows. First, an initial estimate of the variables $A, k,$ and θ are obtained based on the detected positions. Then the residual error (3) is calculated for each frame. Based on that, the weight (4) for each frame is determined. The obtained weights are substituted into (2), and the resulting error function E is minimized over $A, k,$ and θ to get a new estimate of the parameters. This procedure repeats until convergence is reached.

After the heart trajectory is fitted, those image frames in which the distances of the detected heart positions to the trajectory are greater than a threshold are identified. The heart positions in these frames need to be refined. Since the trajectory provides an approximate heart position for these frames, the procedure in section 2.1.2 above is applied again to a small neighborhood of these predicted heart positions. An improved heart position is then returned for each of these frames.

2.1.4. Determining heart's bounding circle

After the heart's center is localized, the next step is to determine the bounding circle of the heart. The bounding circle is the minimum circle circumscribing the heart. Starting from the heart center, we grow a circle and computing the average intensity within the circle for each image frame. Since the heart count is usually higher than the surrounding structure, and since the heart shape is nearly circular, the mean intensity will start to increase initially. However, as the circle passes through the middle of the left ventricle ring, the average intensity within the circle will start to decrease, This is true, even in the presence of non-heart structures of high intensity. This is because these high intensity structures do not have a circular shape and are not centered at the heart center. Based on this property, we can determine the heart's outer bounding circle as the one where the average intensity falls below some pre-defined percentage of the maximum average intensity. A more accurate method for determining the heart size would be to find the reflection point in the intensity profile. This is the point where the second derivative shows maximum. Since the heart is usually not clearly visible at the beginning and the end of the image sequence, and since the heart shape at those places are non-circular, we pick only middle 1/3 of the frames for this analysis. The final heart size is computed as the average of the heart sizes in those middle frames.

2.2. Quantifying the liver-heart effect

2.2.1. Non-Heart activity segmentation

From the bounding circles, the average level of the heart activity (intensity) across all the frames can be computed. Non-heart activities, such as liver, whose intensity level are near or above the average heart activity and whose location are within certain range of distance from the heart, will have interference with the heart in 3D reconstruction. These non-heart activities should be segmented. Since the average heart activity has been computed, the segmentation can be done by setting a threshold near the average heart activity. Pixels whose intensities are above the threshold and are lying outside of the bounding circles are segmented as non-heart activities.

2.2.2. Quantification of the liver-heart effect per frame

The strength of liver-heart artifact depends on several factors. First, the higher the level of non-heart activities, the stronger the liver-heart artifact. Secondly, non-heart activities that are closer to the heart will have greater negative effects. Thirdly, the artifact is proportional to the size of the non-heart activities. Based on these relationships we propose to quantify the degree of liver-heart artifact at the *i*-th frame by the following formula:

$$Q_i = \frac{weighted\_liver\_intensity}{average\_heart\_intensity} \cdot \frac{number\_liver\_pixels}{heart\_area} \cdot \frac{\sum distance(liver\_pixels, heart)}{normalization\_factor} \tag{5}$$

where

$$weighted\_liver\_intensity = \frac{\sum_n I_n w_n}{\sum_n w_n}$$

The variable I_n is the intensity level of the n-th non-heart pixel, w_n is the weight assigned to this pixel, which is computed as being inversely proportional to the distance of the pixel to the heart. The value of the variable Q_i is normalized to lie between 0 and 1. A low values means less liver-heart cross-talk, while a value near 1 indicates a strong liver-heart interference.

2.2.3. Fusion of the measurements

Based on (5), the liver-heart cross-talk of the *i*-th frame can be quantified. The quantifications for all the frames need to be integrated to give a single number indicating the overall quality of the image sequence. Since liver-heart cross-talk usually occurs for consecutive frames, we make local average of the measurements $\{Q_i\}$ to remove any spurious measurement errors. The size of the average window is chosen to be 5. The final quality number is chosen to be the maximum of the smoothed measurements. The above procedure of fusing individual measurements to get the final quality number can be expressed by the following form:

$$Q = \max\{\sum_{k=-2}^{2} Q_i\}$$

In fact, many other forms of integration can be equally applicable. For example, instead of local averaging, the median of the liver activities on a segment of frames can be used.

The quality number obtained can be used by physicians as a guidance as to whether to take appropriate actions. For example, if the quality number is low, other 3D reconstruction methods, instead of the filtered backprojection method, can be used to reduce the artifacts, at the expense of increased computational complexity.

3.EXPERIMENTS

Figure 3 shows an example of quality measure by the proposed technique. Figure 3 (a) is the original image sequence. Fig3 (b) shows the pseudo-motion map of the image sequence. Fig.3(c) is the extracted pseudo-motion map corresponding to the heart. The upper and lower boundaries of the band in Fig.3(c) are the heart position's upper and lower limits used in the heart detection. Fig.3(d) shows the trajectory fitting procedure on the heart positions in the primary detection. Here the x-axis represents the frame number, the y-axis represents the x-coordinates of the detected positions. It can be seen that even large detection errors can still be corrected based on the fitting. Fig.3 (e) illustrates the detected heart positions shown as bounding boxes overlaid on the heart images. The size of the bounding box reflects the estimated heart size. Fig.3 (f) shows the non-heart activity measurement for all the frames. Fig.3 (g) is the quality number extracted from the curve in (f), shown as a bar. The height of the bar is equal to the value of the quality number.

The method of automatic quantification of liver-heart cross talk has been tested on a database of 156 patients. The correct heart detection rate is 96.6% for all the frames. Most detection errors occur at the end of the image sequence where the heart count has become very low. For the purpose of liver-heart artifact quantification, the end of the image sequence almost plays no role, since the liver activities in those frames are low too. From the 156 image sequences, our algorithm is able to give a very reasonable, intuitively good indication of the actual liver activities in the images.

4.CONCLUSIONS

In this paper, we have presented a first automatic method for quantifying the amount of liver activities in SPECT myocardial perfusion imaging. This is an important step toward image quality control. The method provides physicians a single number indicating the degree of liver-heart cross talk that may occur in the image acquisition. With this quality number, the physicians can take appropriate actives to avoid liver-heart artifacts in the 3D reconstruction. Initial experimental results have been very encouraging. Further clinical test and validation are needed to make it practically useful.

REFERENCES:

1. W. Chang, R.E. Henkin, E. Buddemeyer, "The sources of overestimation in the quantification by SPECT of uptakes in a myocardial phantom: concise communication," *Journal of Nuclear Medicine*, Vol.25, 1984, pp.788-791.
2. R.L. Eisner, D.J. Nowsk, W. Fajman, "Fundamentals of 180° acqusition and reconstruction in SPECT imaging," *Journal of Nuclear Medicine*, Vol.27, 1986, pp.1727-1728.
3. R.L. Eisner, ``Use of Cross-correlation function to detect patient motion during SPECT imaging", *Journal of Nuclear Medicine*, Vol.28, No.1, 1987, pp.97-101.
4. G.Q. Wei, J. Qian, E. Chen, J. Engdahl, "A Three-pass Variable-length Correlation Method for Motion Correction in SPECT Myocardial Perfusion Imaging'' , *Proc. SPIE Medical Imaging*, 2000
5. L. Shepp, B. Logan, "The Fourier reconstruction of a head section," *IEEE Trans. Nuclear Sci*, 21, 1974, pp.21-43
6. G. Germano, T. Chua, H. Kiat, J.S. Areeda, D.S. Berman, "A quantitative phantom analysis of artifacts due to hepatic activity in Technetium-99m myocardial perfusion SPECT studies", *Journal of Nuclear Medicine*, Vol.35, No.2, Feb.1994, pp.356-359.
7. J. Nuyts, P. Dupont, V.van den Maegdenbergh, S. Vleugels, P. Suetens, L. Mortelmans, "A Study of the liver-heart artifact in emission tomography," *Journal of Nuclear Medicine*, Vol.36, No.1, Jan.1995, pp.133-139.
8. L. Shepp, Y. Vardi, J.B. Ra, S. K. Hilal, Z.H. Cho, "Maximum likelihood reconstruction for emission tomography," *IEEE Trans. Medical Imaging*, 1, 1981, pp.113-122
9. K. Lange, R. Carson, "EM reconstruction algorithm for emission and transmission tomography," *J. Computer Assist. Tomog.*, 1984, pp.306-316
10. B. Xu, J. Chou, and J. Qian "Determining the position range of the heart from a sequence of projection images using 1-D pseudo motion analysis", US Patent, 5682887, 1997
11. G.Q. Wei, J. Qian, J. Engdahl, "An Integrated Approach to Brightness and Contrast Normalization in Appearance-based Heart Detection in SPECT", *Proc. SPIE Medical Imaging*, 2002

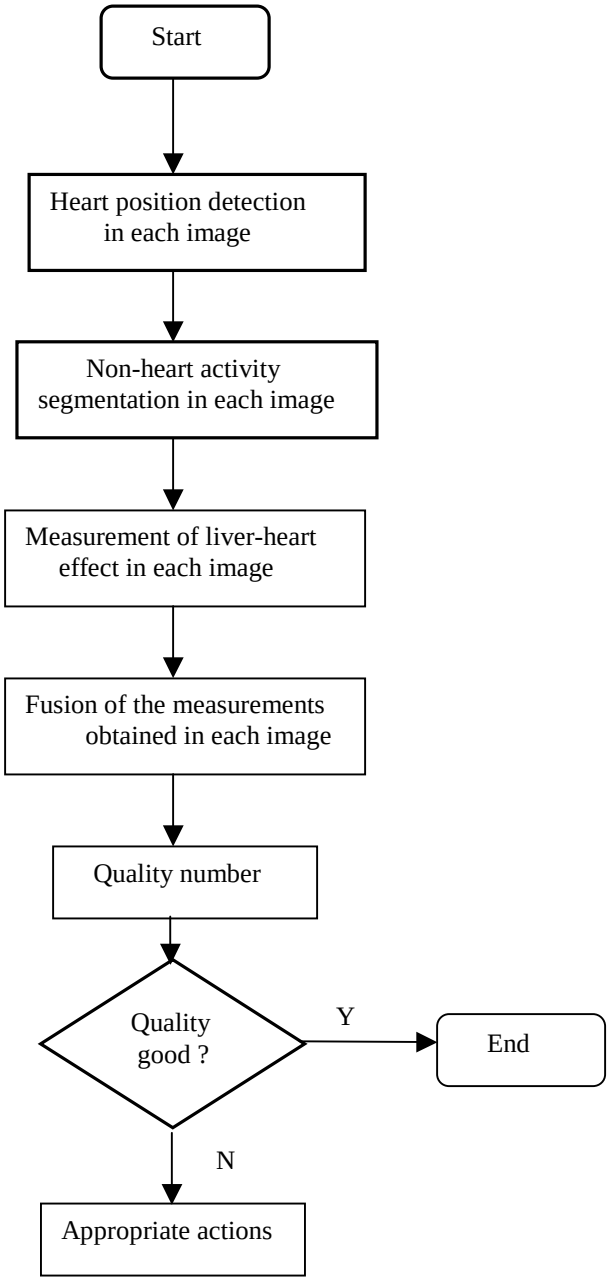

Figure 1: The system diagram of liver-heart artifact quantification.

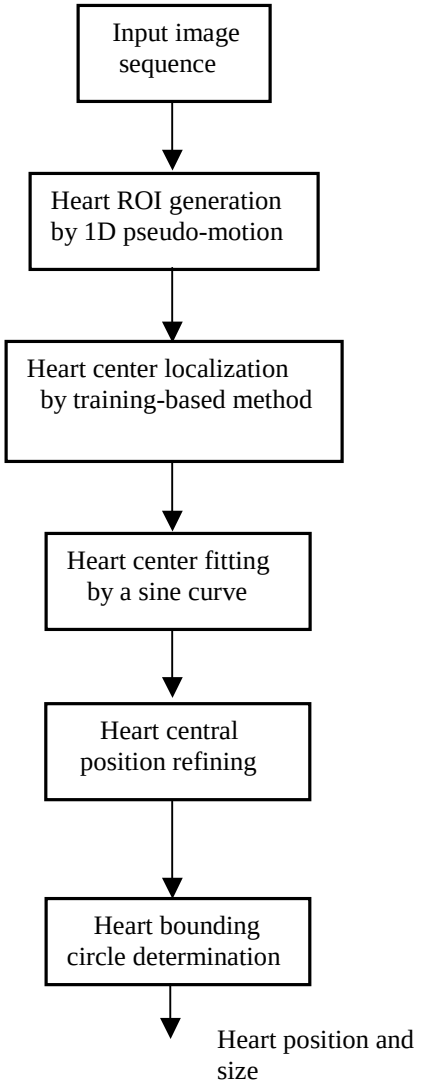

Figure 2: Heart detection with sine curve fitting, outlier detection, and outlier correction.

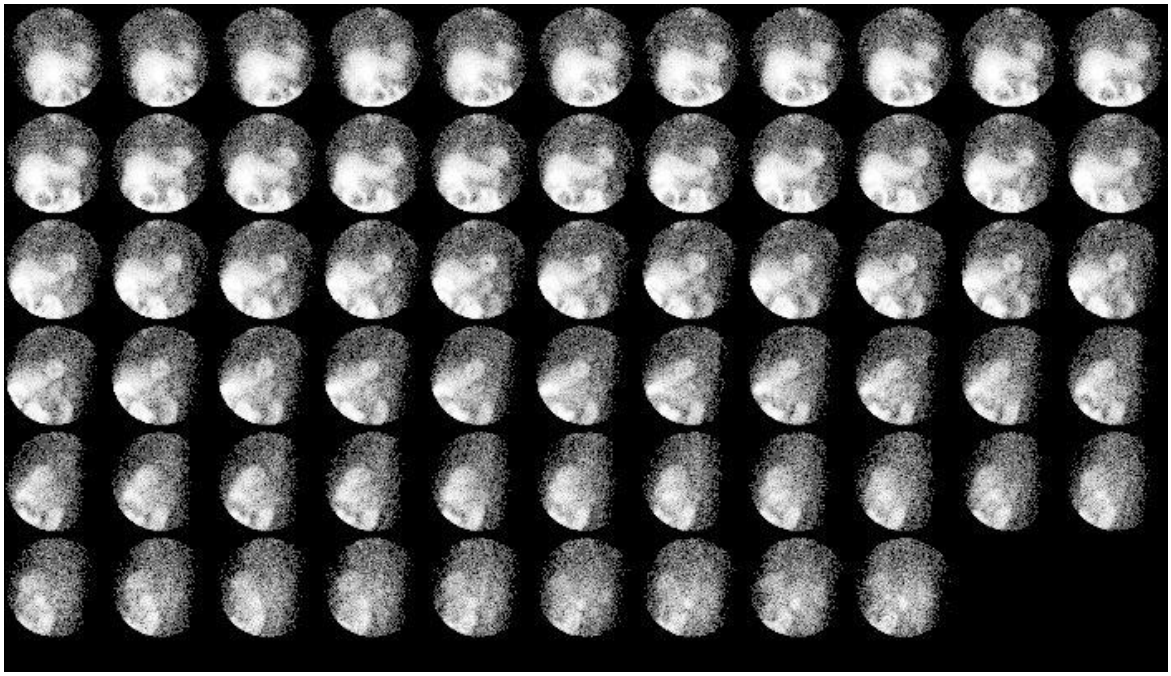

(a)

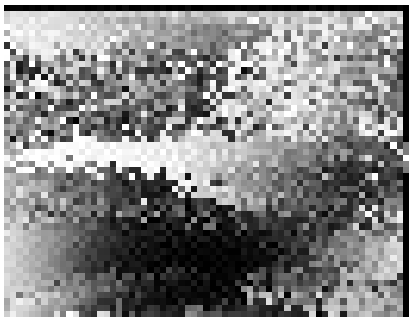

(b)

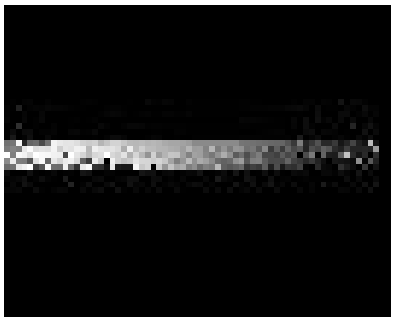

(c)

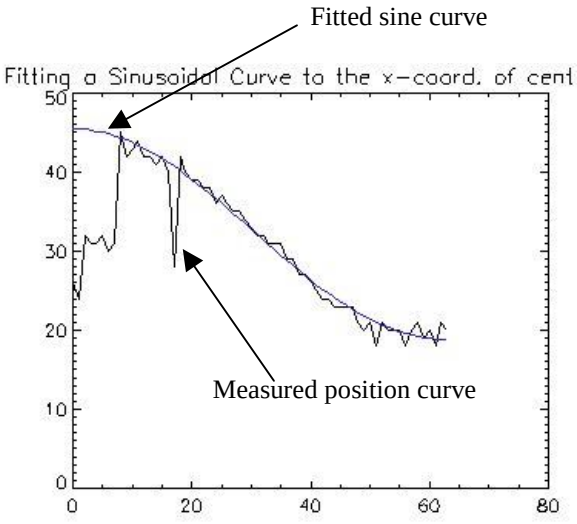
Fitted sine curve
Fitting a Sinusoidal Curve to the x-coord. of cent
50
40
30
20
10
0
0
20
40
60
80
Measured position curve

(d)

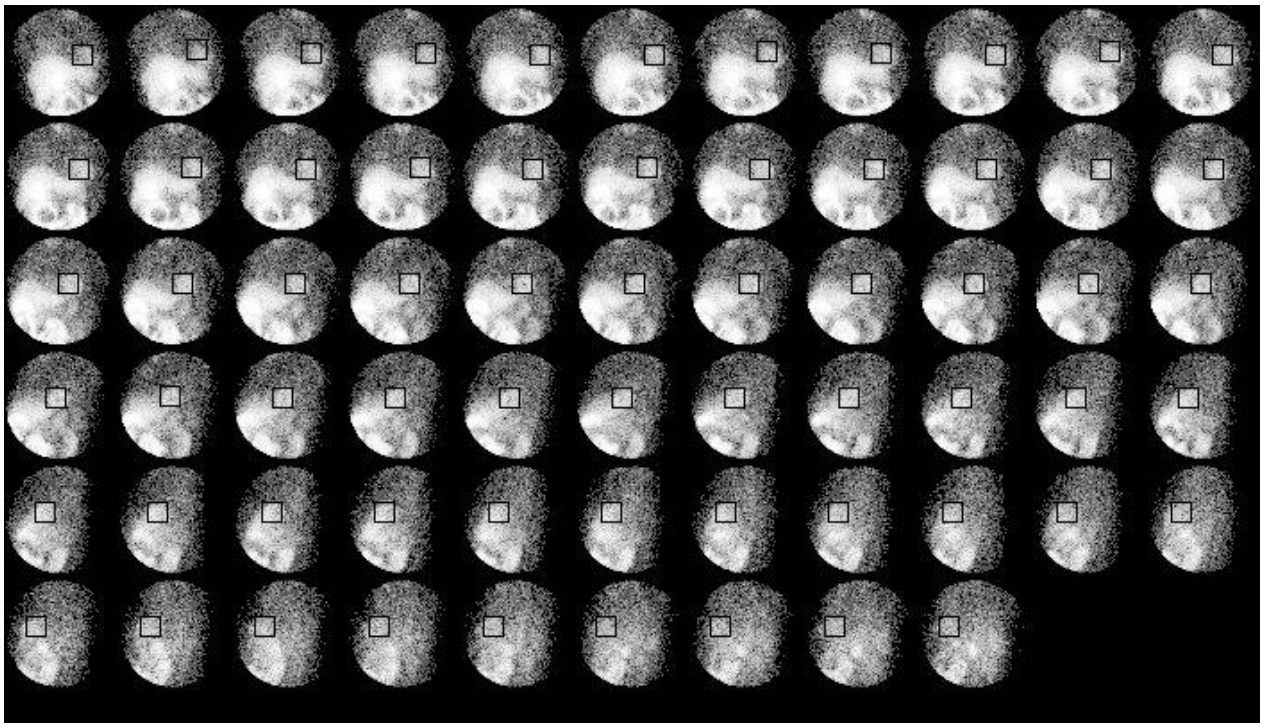

(e)

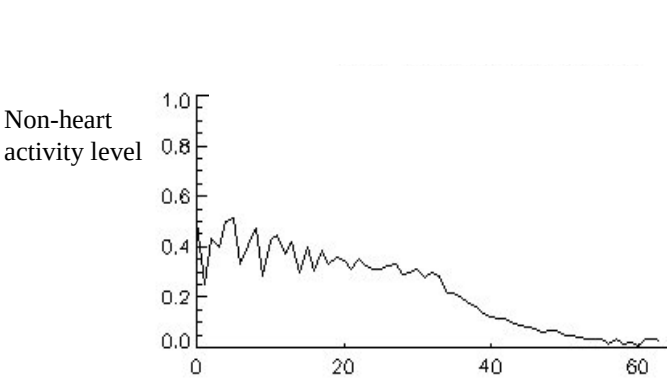

(f)

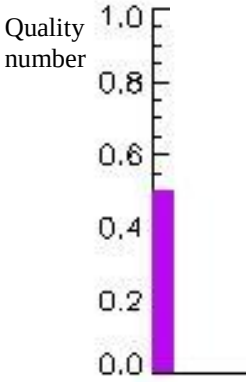

(g)

Figure 3: An example of SPECT image quality measure. (a) original image sequence; (b) pseudo-motion map; (c) extracted pseudo-motion map corresponding to the heart. The upper and lower boundaries of the band are the heart position's upper and lower limits; (d) detected x-coordinates of the heart and the fitted sine curve; (e) detected heart position shown as bounding boxes overlaid on the heart images; (f) non-heart activity measurement for all the frames; (g) quality number extracted from the curve in (f).